ELSEVIER

Chemical Physics 257 (2000) 51–61

Chemical Physics

www.elsevier.nl/locate/chemphys

The isotopic and temperature dependent properties of hydrogen chloride dissolved in carbon tetrachloride. A molecular dynamics approach

G. Chatzis, J. Samios *

Laboratory of Physical and Theoretical Chemistry, Department of Chemistry, University of Athens, Panepistimiopolis 157-71, Athens, Greece

Received 10 February 2000

Abstract

Diluted mixtures of HCl and DCl in CCl_4 were investigated by molecular dynamics simulation technique. The solutions were studied over a wide range of temperatures and at corresponding densities close to coexistence curve of the solvent. The thermodynamical properties obtained are found to be in good agreement with the experiment. The local structure around the solutes was described in terms of the calculated solute–solvent site–site pair distribution functions. We found that, over the entire range of investigation, the effect of density leads to a somewhat slight change of the basic solvation structure around the solute molecules. The behavior of the translational and rotational dynamics of the solutes with density was studied in terms of the center of mass linear velocity and the first-order reorientational autocorrelation functions (ACFs), respectively. We found that the extended Macedo–Litovitz theory [Ricci et al. J. Chem. Phys. 81 (1977) 171] predicts successfully the simulated diffusion coefficients of the solutes at these thermodynamic conditions. Finally, the simulated first-order reorientational ACFs of HCl and DCl were compared to each other as well as to the corresponding experimental ones and a reasonable agreement was obtained.

1. Introduction

In a previous paper [1], hereafter referred as I, we have investigated via molecular dynamics (MD) simulation technique the macroscopic and single dynamical properties of hydrogen chloride (HCl) diluted in carbon tetrachloride (CCl_4) at room temperature.

In our first treatment, we proposed an intermolecular potential model to describe the various molecular interactions in the solution. We have shown that our proposed potential can predict certain properties of the system in quite satisfactory agreement with the experiment.

From the experimental point of view, the dynamics of HCl and DCl in CCl_4 have been the subject of successful infrared (IR) [2–5] and far-infrared (FIR) [6–8] studies in the past. Concretely, Turrell and coworkers [4,5] published IR studies of these solutions and the absorption spectra have been recorded at different temperatures. On the basis of the absorption profiles, Turrell et al. reported and analyzed the first-order reorientational correlation functions (CFs) of

* Corresponding author.
E-mail address: isamios@cc.uoa.gr (J. Samios).

0301-0104/00/$ - see front matter
PII: S0301-0104(00)00133-6

the solute molecules, the spectral moments as well as the root-mean-square (rms) torques and forces acting on the solute molecules.

The work presented here was inspired by the aim to explore the isotopic and temperature (or density) dependent properties of the solute molecules, using a statistical mechanical approach via MD simulation. Therefore, the present work may be regarded as an extension of our first investigation of this solution.

Specifically, we will focus our attention on the structural and dynamical properties of the HCl and DCl solutes in CCl_4 with density, using the potential model reported in our previous study.

To start with, we will concentrate on the thermodynamical properties of the systems as well as the local intermolecular structure close to the solute molecules as a function of temperature or the corresponding density over the whole range of investigation. Particular attention will be paid to the behavior of the translational and reorientational dynamics of the diluted linear solutes in the mixtures with density. Note that a complete description of the well-known interaction induced contributions to the CFs related to the IR and FIR spectra of these solutions will be reported in a subsequent paper. Another objective in this work is to investigate the self-diffusion coefficients of both solute molecules at the present thermodynamical conditions.

Apart from the essential information that successful computer simulations (CS) can provide concerning the properties of molecular systems, previous treatments have shown that these techniques can be employed to check assumptions often used in analytical statistical mechanical theories. Therefore, it makes sense to compare the behavior of the simulated self-diffusion coefficients of HCl and DCl in CCl_4 with results obtained theoretically since we are interested to check theoretical models for the description of the diffusion process of the species in solutions. It has been done here and we will present what we found to be the most promising model for the diffusion of the aforementioned solutes in the solution under investigation.

Since our final goal is to understand better the system properties based upon previous experimental studies and in conjunction with results from CS studies, we have chosen to simulate these solutions at comparable conditions with experiment.

In the following sections, we outline the basic details of the computational method and we present and discuss our predictions. Finally, we summarize the main results.

2. Computational details

As in paper I, the potential model employed in the present simulations was of a site–site pairwise additive type. For the CCl_4–CCl_4 interactions, we used a 5-sites Lennard-Jones (LJ) 12-6 model plus charge–charge electrostatic terms. The HCl–HCl interactions were also represented by a LJ 12-6 potential model using the Laaksonen and Westlund [9] charge distribution, while the HCl–CCl_4 interactions by a site–site exp-6 plus electrostatic terms. The complete description of the potential model is given in Table 1 of our previous MD study of this system. All the MD simulations presented here were carried out in the NVE statistical mechanical ensemble and some of them in the NVT with two solute molecules dissolved in 254 CCl_4 solvents. The thermodynamical state points considered for the simulated solutions were chosen to make possible comparisons with results obtained from the previous experimental studies. Thus, the HCl/CCl_4 solution has been simulated at four different temperatures (253, 273, 290 and 343 K) and solvent densities corresponding to the orthobaric pressure. Note also that the DCl/CCl_4 solution was simulated at the same thermodynamic conditions as the HCl/CCl_4 solution.

In each simulation, a full cut-off radius ($r_c = L_{box}/2$) was applied to all interaction sites between the molecules of the system. Notice that some supplementary MD runs with systems of 496 solvents and four solute molecules have shown no significant differences between the results obtained and those from simulations with 256 molecules. In all cases, the initial configuration was specified by placing the solute molecules close to the center of the simulation box and at an initial separation between 7 and 9 Å with the solvent molecules

Table 1
MD thermodynamic results for the solution HCl/CCl_4 (first line) and DCl/CCl_4 (second line) at various temperatures and molar volumes corresponding to the normal pressure[a]

Run	T_{init} (K)	V_M (cm^3)	T_{sim} (K)	U_{pot} ($kJ\,mol^{-1}$)	P (kbar)
A	253	92.09	257.14	−34.461	0.107 ± 0.363
			252.06	−34.532	0.037 ± 0.343
B	273	94.34	272.61	−33.337	0.039 ± 0.222
			272.12	−33.386	0.009 ± 0.304
C	290	96.50	287.44	−32.335	-0.033 ± 0.140
			289.99	−32.294	0.001 ± 0.135
D	343	102.3	337.64	−29.810	-0.065 ± 0.193

The experimental U_{pot}^{exp} for liquid CCl_4 at 290 K is $-32.20\ kJ\,mol^{-1}$ [10,11]. Estimated error for the simulated average temperature is ±3 K and for the potential energy is $\pm 0.2\ kJ\,mol^{-1}$.
[a] Depicted are the initial temperature, the molar volumes and the equilibrium estimated properties: temperature, T; potential energy, U_{pot}; and the pressure, P (mole fraction $X_{HCl} = X_{DCl} \cong 0.008$).

randomly distributed around the solutes. Note also that the initial orientation of all the solute and solvent molecules were selected randomly.

3. Results and discussion

3.1. Thermodynamical and structural properties

The calculated average potential energy, U_P, and pressure, P, of both diluted mixtures (HCl/CCl_4, DCl/CCl_4) at various temperatures and corresponding molar volumes, are depicted in Table 1. Despite the fluctuations obtained, the simulations yield small pressures within the error bars as they should. On the other hand, the estimated mean configurational energies are found to be in good accordance with the experimental results for the pure liquid CCl_4 in the relevant range of densities. For comparison, the experimental value of U_P^{exp} for liquid CCl_4 at 290 K is $-32.20\ kJ\,mol^{-1}$ [10–12], while the MD predictions are -32.335 and $-32.294\ kJ\,mol^{-1}$ for HCl/CCl_4 and DCl/CCl_4, respectively. Note also that the energetic results calculated at high and low temperatures provide an acceptable behavior of this property as a function of temperature. The experimental potential energy, U_P^{exp}, was obtained from the heat of vaporization ΔH_{vap}^{exp} according to the well-known relation:

$$U_P^{exp} \approx -\Delta H_{vap}^{exp} + RT. \quad (1)$$

In what follows, we turn our attention to the intermolecular structure of the system under study.

As mentioned in Section 1, another important and closely related aspect to the solute dynamics concerns the extent over which the temperature or density affects the local structure of the solute (HCl or DCl) molecules in the solutions. Unfortunately, experimental results from diffraction studies concerning the local structure of HCl in liquid CCl_4 are not available in the literature. Note, however, that in our first treatment, the overall system structure at 290 K has been well described and analyzed in terms of the calculated relevant atom–atom pair distribution functions (PDFs). We, therefore, omit here any extensive discussion concerning the behavior of these functions in detail. Thus, our discussion will be limited mainly to a comparison of the calculated PDFs for the HCl/CCl_4 at the two extreme state points, namely at 253 and 343 K and corresponding densities. Note that at each state point, the behavior of DCl/CCl_4 PDFs were found to be quite similar to those of HCl/CCl_4 system.

The characteristic extrema of all these PDFs as well as the average coordination numbers at state points A and D are displayed in Table 2. The most interesting short-range parts of these PDFs related to the solvation structure of HCl are also presented in Fig. 1a–e.

As we can see from the figures and Table 2, for a given PDF, the first peak changes in amplitude and in position when the temperature is varied, whereas the second peak (not shown in Fig. 1) also

Table 2
Positions and heights of the first maximum and minimum in the calculated PDFs (r (Å):$G(r)$) and the coordination numbers for the first solvation shell around the solute (HCl) molecule at 253 K (first line) and 343 K (second line)

$G(r)$	I. Maximum		I. Minimum		Coordination number	
	Position (Å)	Amplitude	Position (Å)	Amplitude	I. Maximum	I. Minimum
COM(a)–COM(b)	4.50	2.349	6.70	0.610	1.717	8.464
	4.60	2.158	6.50	0.703	1.774	7.256
Cl(a)–C	4.50	2.327	6.70	0.615	1.780	8.464
	4.60	2.152	6.50	0.765	1.776	7.265
H–C	4.20	1.769	7.00	0.734	1.289	9.281
	4.20	1.647	7.00	0.782	1.142	8.522
Cl(a)–Cl(b)	3.60	2.046	5.00	0.832	3.554	12.976
	3.70	1.830	5.20	0.889	2.980	12.817
H–Cl(b)	4.70	1.109	6.40	0.998	10.164	28.499
	4.90	1.166	6.70	0.963	10.576	29.550
Plateau on the $G_{\mathrm{H-Cl(b)}}(r)$	3.00	0.936	–	–	1.310	–
	3.60	0.971	–	–	3.431	–
	3.00	0.852	–	–	1.064	–
	3.60	0.916	–	–	2.831	–

display a somewhat slight change for all the PDFs, as they should. The changes observed in the PDFs give us a hint as to a small structural change taking place in the system and specifically around the solute molecule from the state point D (low density) to the state point A (high density). Note, however, that the characteristic shoulder on the right-hand side of the $G_{\mathrm{H-Cl(b)}}(r)$ function seems to be retained in the solution at high and low density. Therefore, from the above results, it appears that the effect of density leads to a more or less compact rearrangement of the solvent molecules around the solute molecule and essentially to a not dynamic change of the basic solvation structure.

As in our first study of this solution, by inspecting the calculated coordination numbers at state points A and D, one may conclude that a number of Cl (CCl_4) atoms are relatively in contact with the HCl molecule. These atoms construct the walls of a dynamical cage in which the solute molecule rotates and translates freely until its first collision take place with the wall atoms. It is found that on an average the solute *cavity* is constructed by a maximum of six to seven Cl (CCl_4) atoms at the highest density (A) and by about five to six Cl (CCl_4) atoms at the lowest investigated density (D).

As can be seen below, this slight modification of the solute cavity from one state point to another seems to be sufficient for a noticeable change concerning mainly the dynamical properties of the solute molecules.

3.2. Translational dynamics and transport properties

The translational motion of HCl and DCl diluted in CCl_4 was studied at each state point of interest and in terms of the appropriate time correlation functions (TCFs) of the COM linear velocity autocorrelation functions (vACFs) $C_{\mathrm{v}}^{\mathrm{HCl}}(t)$ and $C_{\mathrm{v}}^{\mathrm{DCl}}(t)$. The results obtained are shown in Fig. 2a–d. Fig. 2a illustrates the behavior of the $C_{\mathrm{v}}^{\mathrm{HCl}}(t)$ functions obtained at 253, 273, 298 and 343 K. The $C_{\mathrm{v}}^{\mathrm{DCl}}(t)$ correlations are presented in Fig. 2b. The vACFs of HCl and DCl obtained at 253 and 298 K are compared to each other in Fig. 2c and d, respectively. The correlation times were evaluated by integrating the corresponding functions up to 2 ps and they are shown in Table 3.

Another interesting quantity which has been calculated is the rms force $\langle F^2\rangle^{1/2}$ acting on the solute due to its surrounding solvent molecules. The results obtained for this property are depicted in Table 3. The present MD finding is found to be

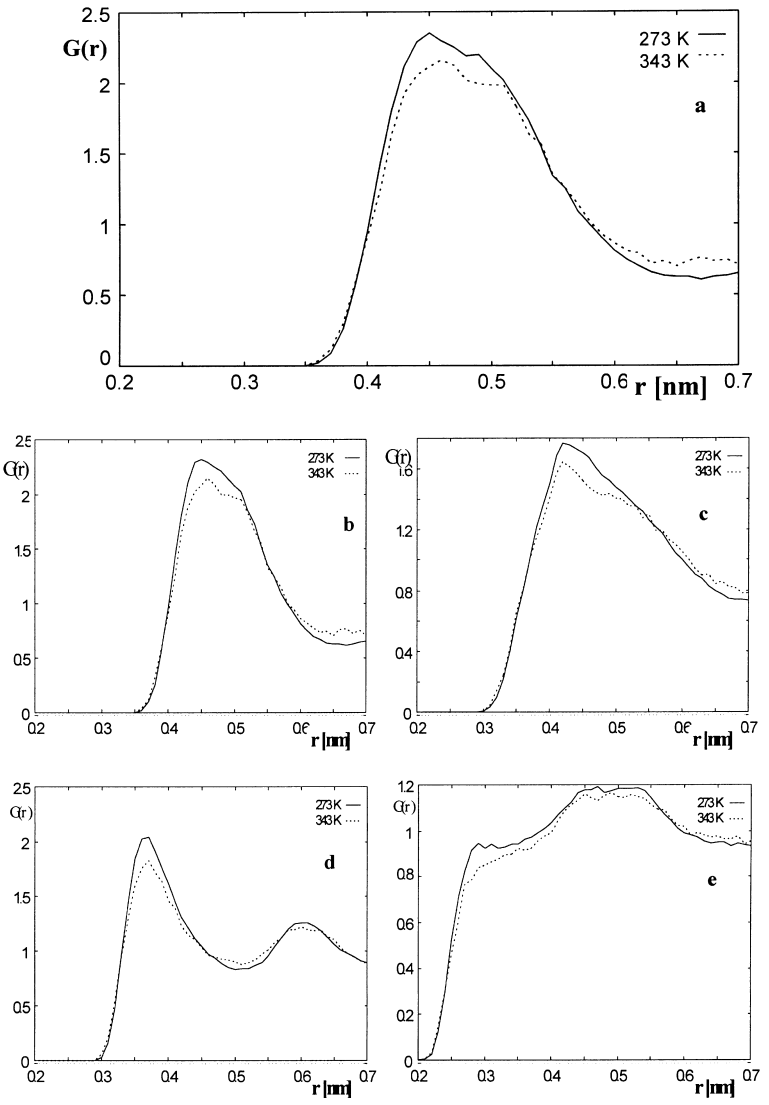

Fig. 1. Center of mass and atom–atom pair distribution functions $G(r)$ for the solution HCl/CCl_4 (a = HCl, b = CCl_4) at 253 K (solid lines) and 343 K (dashed lines): (a) COM–COM $G_{a-b}(r)$, (b) $G_{Cl-C}(r)$, (c) $G_{H-C}(r)$, (d) $G_{Cl(a)-Cl(b)}(r)$, and (e) $G_{H-Cl(b)}(r)$.

comparable with previously reported behavior of rms force data estimated from the second and fourth moments of the IR spectral profiles [5] on the basis of well-known theoretical expression [4,5].

By inspecting the curves displayed in Fig. 2a and b, we may observe that they show the well-known behavior of the translational motion, as in the case of simple liquids. From Fig. 2a, we see that the initial decrease of vACF is more rapid at higher densities. For the highest density (state point A), e.g., it rapidly reaches zero in less than 0.2 ps and exhibits a negative minimum of −0.18 at 0.28 ps. The curve shows a long anticorrelation region and converges to zero after about 1.5 ps. The vACF curve of HCl at the lowest density (state point D) goes through a more shallow negative minimum than the other three curves and

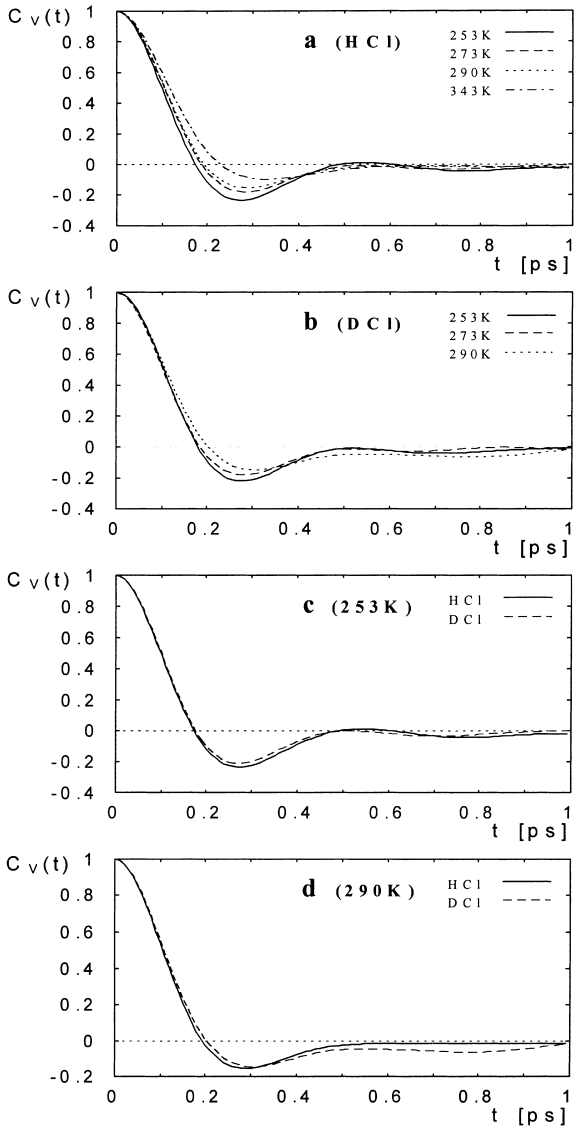

Fig. 2. TCFs for the COM linear velocity for the solute molecules HCl and DCl at various temperatures and corresponding densities (state points A, B, C, D) from this MD study: (a) vACFs for HCl, (b) vACFs for DCl, (c,d) comparison of vACFs for HCl (—) with DCl (– – –) at state points A and C.

after that converges to zero. As the density decreases, the negative minima of the vACFs are shifted to somewhat larger times. As we can see from Fig. 2b, the vACFs for DCl follow a similar course with density compared to the vACFs for HCl. However, by comparing the HCl function with that for DCl at the same state points, we may observe small differences concerning their time evolution. At very short times, the HCl curves decrease faster than the curves of DCl. At larger times, however, the DCl vACFs are the more negative and lived functions. Obviously, this negative, deep and relatively long tails in these functions lower the value of their integrals.

As mentioned in Section 1, the evaluation of the self-diffusion coefficients D_s^x (x = HCl or DCl) of the solute molecules in the sample is also included in the framework of the present MD treatment. In CS studies, the self-diffusion coefficients may be calculated from the equilibrium linear velocity CFs:

$$D = \frac{1}{3}\int_0^\infty \mathrm{d}t \left\langle \vec{v}_i(0)\cdot\vec{v}_i(t)\right\rangle, \tag{2}$$

or alternatively, by using the well-known Einstein relation [13]

$$6D = \lim_{t\to\infty}\frac{1}{t}\left\langle [\Delta r_i(t)]^2\right\rangle. \tag{3}$$

In the present study, the above quantities of interest are evaluated using the mean squared displacements (MSD) method. Uncertainties subjected to the periodic boundary conditions were also investigated. We notice furthermore that our results were obtained on the basis of relatively long MSD plots of about 80 ps from which only the last 40 ps were used for the estimation of the coefficients.

As can be observed from the diffusion data selected in Table 3, the calculated self-diffusion coefficients D_s^{HCl} and D_s^{DCl} show a non-linear temperature dependence. They increase with increasing temperature of the system. Moreover, the self-diffusion coefficients of the solvent molecules $D_s^{CCl_4}$ were also calculated and the results are displayed in Table 3. Further, the CCl_4-MD diffusion values depend non-linearly on temperature over the whole range of investigation. Unfortunately, experimental data for the diffusion coefficients of both species in this highly diluted mixture are not available. In this case, it is very interesting to compare our results for the HCl/CCl_4 system with

Table 3
Correlation times τ_c (ps) of the linear velocity, **u**, the P_1, P_2 Legendre polynomials ACFs, the rms force as well as the self-diffusion coefficients of the HCl/CCl_4 (first line) and DCl/CCl_4 (second line) at state points A–D[a]

T (K)	τ_u	τ_1	τ_2	$\langle F^2\rangle^{1/2}$ (10^{11} cm^{-2})	D_s^{HCl} (10^{-9} m^2 s^{-1})	$D_s^{CCl_4}$ (10^{-9} m^2 s^{-1})
A	0.049	0.230	0.107	1.50	1.9659	0.7775
	0.058	0.342	0.174	1.44	1.3108	
B	0.052	0.214(0.205)	0.094	1.51	2.7511	1.0518
	0.064	0.327(0.270)	0.126	1.48	2.1770	
C	0.056	0.190(0.189)	0.086	1.51(1.62)	3.3997	1.4348
	0.072	0.223(0.241)	0.100	1.49	2.7167	
D	0.091	0.147(0.160)	0.050	1.56	7.4063	2.3763

[a] The numbers in parentheses denote experimental data [5].

MD results for similar mixtures obtained by other authors. We mention, e.g., the mixtures of $CHCl_3/CCl_4$ which have been studied by MD calculations [14] based on (18-6) LJ type potentials. It is found that the solvent diffusion coefficients calculated in the case of the above-mentioned diluted mixtures are comparable. Additional diffusion data of various small species as constituents in solutions can be also found in Refs. [15,16].

It is worthwhile to note that the self-diffusion data of many molecular systems along the liquid side of the coexistence curve can be interpreted by a simple two parameter exponential type equation,

$$D_s(T) = D_0 \exp(-\Delta E/RT). \tag{4}$$

Both D_0 and ΔE are temperature independent parameters, and Eq. (4) can be compared with an Arrhenius type equation for the dependence of a chemical rate constant. For many years, this fact led many authors [17] to describe the diffusion process in liquids as an activated one, and the parameter ΔE occurring in Eq. (4) has been interpreted as an activation energy. However, as pointed out by several workers, the temperature dependence in the behavior of the self-diffusion coefficients along the coexistence curve is essentially due to the work done in reducing the density from a given temperature to a higher one. Macedo and Litovitz (ML) [18,19], e.g., have assumed that the value of the transport coefficients must depend both on density and on energy fluctuations. ML [18] write $D = D_0 P_V P_E$, where P_V is the probability that enough free volume is present in the system and P_E, the probability the molecules to have enough energy so that they can diffuse with small and random displacements. According to this idea, Eq. (4) can be extended to the following expression:

$$D(V,T) = D_0 \exp\left(-\gamma \frac{V_0}{V - V_0} - \frac{E^*}{RT}\right). \tag{5}$$

D_0 is taken to be constant, γ denotes a numerical factor and E^*, the energy threshold value to allow diffusion. V_0 is the excluded (close-packed, $V_0 = N\sigma_s^3/2^{1/2}$) molar volume. V_0 depends only on the solvent properties, i.e. the hard-sphere diameter of the solvent σ_s, since in the case of a dilute mixture the concentration of the solute molecules is practically zero.

Ricci et al. [19] expressed the ideas of ML not by Eq. (5), but as follows:

$$D(V,T) = C D_{HS}(V,T) \exp\left(-\frac{E^*}{RT}\right), \tag{6}$$

where C is a numerical factor. $D_{HS}(V,T)$ denotes the hard-sphere self-diffusion coefficients.

At this point, it is interesting to mention that in the case of a dilute mixture Ricci et al. were able to extend Eq. (6) in order to describe the diffusion process of the impurity in the solution. In this case, E^* must depend both on solute–solvent and on solvent–solvent interaction. According to the extended theory, and for densities in the range of $1.6 \leqslant V/V_0 \leqslant 3$, the diffusion of the impurity can be expressed as follows:

$$D(V,T) = CA(\sigma')\sqrt{\frac{T}{M_s}}\left(\frac{M_s}{M_T}\right)^{0.5-\alpha} V_0^{1/3} \times \exp\left(-\frac{\gamma(\sigma')V_0}{V-V_0} - \frac{E^*}{RT}\right). \quad (7)$$

$A(\sigma')$, $\gamma(\sigma')$ and α are given in Fig. 3 and Table 1 in Ref. [19]. M_s/M_T is the solvent–solute mass ratio.

In Fig. 3, we report the comparison between the simulated diffusion coefficients and the theory via Eq. (7) by using $\gamma(\sigma') = 1.5$, $A(\sigma') = 12 \times 10^{-5}$, $\alpha = 0.29$ and $V_0 = 60$ cm^3 mol^{-1} taken from Ref. [19]. E^* is determined for each case by fit. As we can see, the extended ML theory predicts successfully the simulated self-diffusion coefficients of HCl and DCl in CCl_4. In the case of HCl/CCl_4, the estimated E^* was found to be 604.3 cal mol^{-1}, while for the DCl/CCl_4 was 696.6 cal mol^{-1}. Note that in the case of the pure liquid CCl_4, Ricci et al. estimated the above energy to be 680 cal mol^{-1} [19].

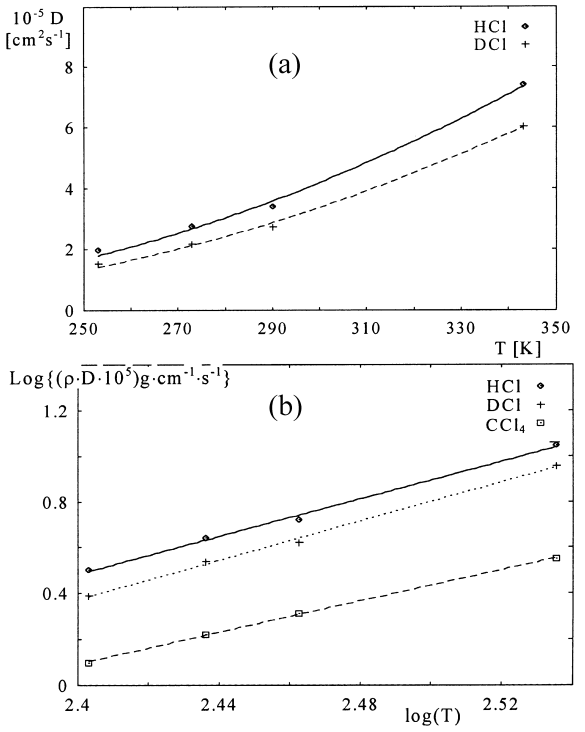

Fig. 3. Temperature dependence of the self-diffusion coefficient of the solute molecules: (a) direct plot of the self-diffusion coefficient of HCl and DCl versus temperature and (b) logarithmic plot of the product of self-diffusion coefficient with corresponding density of the mixture. For comparison we present the one for the mixture solvent.

Another point of particular interest here is the fact that, using the orthobaric densities ρ from the PVT data of the system and the D_s^x (x = HCl or DCl) values from the present simulations, we found out that a relationship of the following type holds:

$$\rho D_s^x(T) = AT^a, \quad (8)$$

where A and a are constants. It may be verified from the plot shown in Fig. 3b in which we have plotted the quantity $\log[\rho D(T)]$ versus $\log T$. Note also that Ricci and Rocca [20] pointed out that Eq. (8) gilds in many ordinary liquids. They pointed out that the values obtained for the parameter a are very close to the number 2.7. In our case and for the data D_s^{HCl}, D_s^{DCl} and $D_s^{CCl_4}$, we find straight lines with slopes $a_{HCl} = 4.2$, $a_{DCl} = 4.3$ and $a_{CCl_4} = 3.2$, respectively.

3.3. Rotational dynamics of HCl diluted in CCl_4

The single-molecule reorientational motion of the probe molecules (HCl or DCl) in the sample was studied at each thermodynamic state point of interest and in terms of the most important first- and second-order Legendre ACFs:

$$C_1^x(t) = \left\langle \hat{u}_i^x(0) \cdot \hat{u}_i^x(t) \right\rangle \quad (9)$$

$$C_2^x(t) = \left\langle 1.5\left|\hat{u}_i^x(0) \cdot \hat{u}_i^x(t)\right|^2 - 0.5 \right\rangle. \quad (10)$$

$\hat{u}_i^x$ represents the unit vector along the molecular axis of the solute molecule i (x = HCl or DCl).

As mentioned in Section 1, the reorientational motion of HCl in CCl_4 has been investigated experimentally by several groups in the past. Therefore, it is of great interest here to check on how well the proposed potential model predicts the experimentally accessible first-order ACFs of HCl and DCl in CCl_4 with temperature. Fig. 4a and b shows the behavior of the simulated $C_1(t)$ ACFs of the solute molecules in the mixtures with temperature. We may observe that the $C_1(t)$ curves exhibit a minimum, followed by a submaximum and

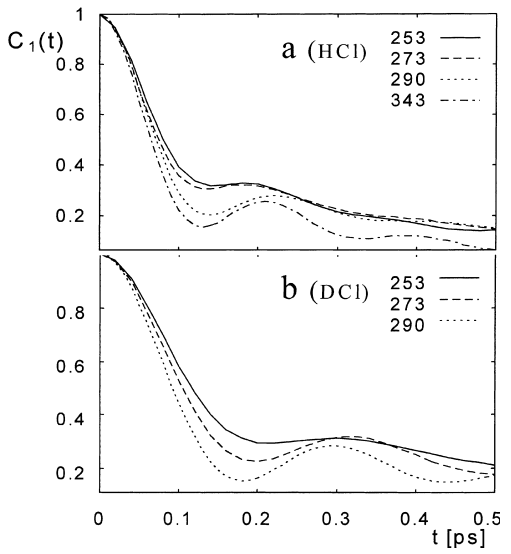

Fig. 4. First-order Legendre polynomials temperature behavior: (a) HCl and (b) DCl at state points A, B, C, and D.

subsequently they approach zero after long times. In addition, the $C_1(t)$ curves are shifted to higher ordinate values (slower decay) with decreasing temperature. This behavior is due to the increasing steric effects of the solvent molecules with increasing density. The estimated single-molecule reorientational correlation times τ_1 are depicted in Table 3 together with the corresponding IR [5] relaxation times. The agreement between the experimental and simulated reorientational times τ_1 is remarkably good. Also, the comparison of the computed $C_1(t)$ ACFs with the corresponding IR reorientational ACFs shows clearly that the shape of the experimental functions is quantitatively reproduced not only at short but also at intermediate and long times.

The second-order Legendre reorientational ACFs of the solute molecules are not available in the literature. Therefore, a direct comparison of the simulated $C_2(t)$ ACFs (not shown here) with experiment is impossible at the present time. The estimated single-molecule reorientational correlation times τ_2 are also depicted in Table 3.

From Table 3, we see that the calculated correlation times τ_1 and τ_2 decrease with increasing temperature of the system. This MD result is in accordance with the experiment. On the other hand, it is well known that the ratio between the corresponding reorientational times τ_1 and τ_2 is an indication for the type of the reorientational diffusion motion of the molecules in the sample. Thus, for a rotational molecular process with relatively small angular steps, the well-known Hubbard relation ($\tau_1 = 3\tau_2$) is fulfilled and the rotational motion can be treated as a diffusional one. When the rotational motion consists of larger angular steps, the (τ_1/τ_2) ratio is expected to be quite smaller than 3. This is what we observe from the MD reorientational times τ_1 and τ_2 of HCl as well as of DCl dissolved in CCl_4. Notice that in all cases, the above-mentioned ratio is found to be closer to 2 than to 3.

It is also interesting to note that the comparison of the computed $C_1(t)$ ACF of HCl with that of DCl in CCl_4 at a given temperature in Fig. 5 yield an isotopic shift of the latter curve relatively to the former. However, in studying isotopic dynamical effects, it is convenient to introduce a reduced time variable t^* defined by $t^* = t(KT/I)^{1/2}$ and then to compare appropriate CFs for the isotopic species at a given temperature. It was done in the present work and some results are shown in Fig. 6, where the ACFs $C_1(t)$ of HCl and DCl at 290 K are plotted against the reduced time. From

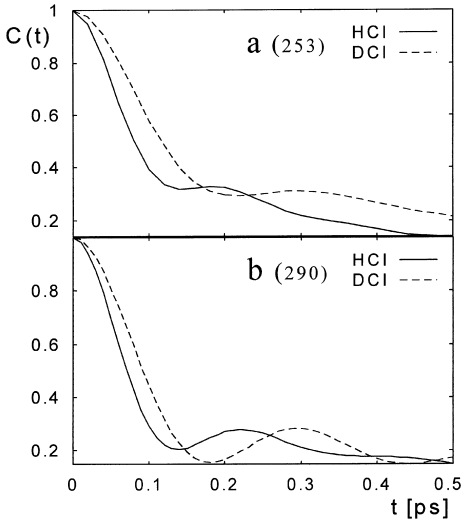

Fig. 5. Isotopic effect in the reorientational motion of the solute molecules. Direct comparison of the $C_1(t)$ for HCl and DCl at (a) 253 and (b) 290 K.

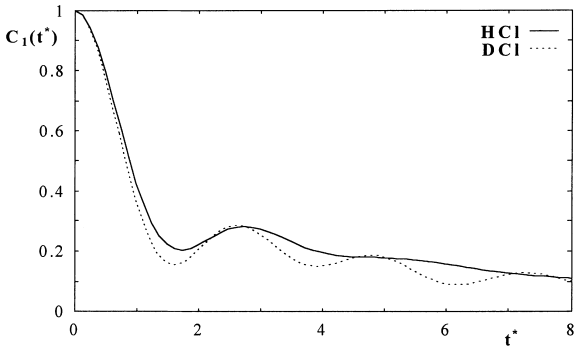

Fig. 6. Comparison of first-order RACFs $C_1(t)$ for HCl and DCl at 290 K plotted with the reduced time t^*.

the corresponding plots in Fig. 6, we see that the two curves become nearly super-imposed at times approximately equal to τ_{min} and in the region of the submaximum. This behavior has also been observed experimentally by Keller et al. [2] and by Turrell et al. [5]. In addition, Turrell et al. based on their IR results pointed out that rotation–translation coupling makes a significant contribution to the dynamics of HCl and DCl dissolved in CCl_4.

4. Conclusions and remarks

An interesting issue in chemical physics of pure liquids and liquid mixtures is the question, namely the dependence of structural, translational and rotational properties (and thus of transport processes) on various thermodynamic variables and on the characteristics of the species which constitute molecular systems. From the experimental point of view, different kinds of suitable experimental techniques allow the study of selective solvation of species in binary mixtures and the investigation of microdynamical properties in solutions. On the other hand, an alternative approach to the answer of these questions is the microscopic simulation of the fluids under controlled conditions. In the present study, we tried to contribute to this question, in the case of HCl and DCl dissolved in CCl_4, using a statistical mechanics approach via molecular dynamics simulations. We have thus calculated quantities, which are experimentally accessible in the real system, and other quantities, which although not directly observable, may be useful in obtaining a further insight into the details of molecular dynamics of the system.

The solutions, HCl/CCl_4, DCl/CCl_4, were simulated at thermodynamic state points close to the coexistence curve of the solvent. Several properties of the system, including thermodynamical, structural, transport and some dynamical properties were obtained and their temperature (density) dependence was presented and discussed. The structural results are presented in the form of the atom–atom pair distribution functions. A close inspection of these functions indicates clearly that the cavities around the solute molecules do not change dramatically when the temperature and consequently the density of the system is varied at the present thermodynamic conditions. Notice that this slight modification of the cage around the solute molecules in the system seems to be very important for the behavior of the translational and rotational dynamics of the probe molecules and thus for the behavior of their transport properties with density. The calculated center of mass linear-velocity and the first-order Legendre reorientational ACFs as well as the self-diffusion coefficients of the solute molecules support this suggestion.

The simulated and experimental $C_1(t)$ reorientational ACFs obtained from previous IR studies were compared at different temperatures. The comparison shows that the shape of the experimental ACFs is quantitatively reproduced.

Finally, we found that the simulated diffusion coefficients of the solute molecules (HCl, DCl) at the present thermodynamic conditions may be successfully reproduced using the extended ML theory according to the previous treatment of Ricci et al. [19].

Acknowledgements

This work was carried out within the project No. 70/4/3394AU. The financial support of the University of Athens is gratefully acknowledged. The CPU time allocation on the Convex machine and on the HP 735 (eight nodes) of the Computing

Center of the University of Athens-Greece is also gratefully acknowledged.

References

[1] G. Chatzis, M. Chalaris, J. Samios, Chem. Phys. 228 (1998) 241.
[2] B. Keller, F. Knenbuehl, Helv. Phys. Acta 45 (1972) 1127.
[3] J. Lascombe, M. Besnard, P.B. Caloine, J. Devaure, M. Perrot, in: J. Lascombe (Ed.), Molecular Motion in Liquids, D. Reidel, Dordrecht, The Netherlands, 1974.
[4] G. Turrell, J. Mol. Spectrosc. 19 (1978) 383.
[5] E.C. Mushayakarara, G. Turrell, Mol. Phys. 46 (1982) 991.
[6] Y. Ohikubo, S. Ikawa, M. Kimura, Chem. Phys. Lett. 43 (1976) 138.
[7] S. Ikawa, K. Sato, M. Kimura, Chem. Phys. 47 (1980) 65.
[8] S. Ikawa, S. Yamazaki, M. Kimura, Chem. Phys. 51 (1980) 151.
[9] A. Laaksonen, P.O. Westlund, Mol. Phys. 73 (1991) 663.
[10] K. Hlavaty, Czech. Chem. Commun. 35 (1970) 2878.
[11] B.S. Harsted, E.S. Tmomsen, J. Chem. Thermodynam. 79 (1975) 369.
[12] Landolt, Börnstein, Zahlenwerte und Funktionen, Springer, Berlin, 1969.
[13] D.A. McQuarrie, Statistical Mechanics, Harper and Row, New York, 1976.
[14] C. Hoheisel, U. Deiters, Ber. Bunsenges. Phys. Chem. 81 (1977) 1225.
[15] C. Hoheisel, Theoretical Treatment of Liquids and Liquid Mixtures, Elsevier, Amsterdam, 1993.
[16] J. Millat, J.H. Dymond, C.A. Nieto de Castro (Eds.), Transport Properties of Fluids: Their Correlation, Prediction and Estimation, Cambridge University Press, Cambridge, 1996.
[17] H.J.V. Tyrrell, K.R. Harris, Diffusion in Liquids, Butterworths, London, 1989.
[18] P.B. Macedo, T.A. Litovitz, J. Chem. Phys. 42 (1965) 245.
[19] F.P. Ricci, M.A. Ricci, D. Rocca, J. Chem. Phys. 81 (1977) 171.
[20] F.P. Ricci, D. Rocca, in: A.J. Barnes, W.J. Orville-Thomas, J. Yarwood (Eds.), Proc. of the NATO Advanced study Institute on Molecular Liquids – Dynamics and Interactions, Florence, 1983, p. 35.